RSC Advances

PAPER

View Article Online
View Journal | View Issue

Cite this: *RSC Adv.*, 2020, **10**, 8735

Core size does not affect blinking behavior of dye-doped Ag@SiO_2 core–shell nanoparticles for super-resolution microscopy†

S. Thompson and Dimitri Pappas *

Dye-doped nanoparticles have been investigated as bright, luminescent labels for super-resolution microscopy *via* localization methods. One key factor in super-resolution is the size of the luminescent label, which in some cases results in a frame shift between the label target and the label itself. Ag@SiO_2 core–shell nanoparticles, doped with organic fluorophores, have shown promise as super-resolution labels. One key aspect of these nanoparticles is that they blink under certain conditions, allowing super-resolution localization with a single excitation source in aqueous solution. In this work, we investigated the effects of both the Ag core and the silica (SiO_2) shell on the self-blinking properties of these nanoparticles. Both core size and shell thickness were manipulated by altering the reaction time to determine core and shell effects on photoblinking. Size and shell thickness were investigated individually under both dry and hydrated conditions and were then doped with a 1 mM solution of Rhodamine 110 for analysis. We observed that the cores themselves are weakly luminescent and are responsible for the blinking observed in the fully-synthesized metal-enhanced fluorescence nanoparticles. There was no statistically significant difference in photoblinking behavior—both intensity and duty cycle—with decreasing core size. This observation was used to synthesize smaller nanoparticles ranging from approximately 93 nm to 110 nm as measured using dynamic light scattering. The blinking particles were localized *via* super-resolution microscopy and show single particle self-blinking behavior. As the core size did not impact blinking performance or intensity, the nanoparticles can instead be tuned for optimal size without sacrificing luminescence properties.

Received 11th December 2019
Accepted 19th February 2020

DOI: 10.1039/c9ra10421f

rsc.li/rsc-advances

Introduction

Bright nanoparticles based on metal-enhanced fluorescence have shown promise as probes for super-resolution microscopy.[1] Labels with high brightness allow for an improved localization precision through methods such as STochastic Optical Reconstruction Microscopy (STORM) and related methods.[2–5] In the case of nanoparticle labels, an added benefit is that some of these nanostructures can undergo a self-induced blinking, or switching between "on" and "off" states.[1,6–9] Self-blinking eliminates the need for photoswitchable probes and multiple excitation sources, potentially simplifying STORM microscopy instrumentation. Most organic dye molecules currently in use need to be stimulated to turn on and off, which requires complex equipment setups. In addition, localization precision increases with photon count. The dye doped nanoparticles cycle between the on and off states on their own, removing the need for complex equipment setup. They are also potentially much brighter than single fluorophores, thus improving localization.

In photoblinking, the duty cycle of the reversible self-switching between "on" and "off" states is an important aspect of nanoparticle design.[6,10–14] In recent years many blinking nanostructures made from varying materials such as carbon dots, polymer dots, organic dyes, photoswitchable fluorescent proteins, and fluorescent nanoparticles have been studied.[15–17] The duty cycle and intensity during the "on" states are critical parameters in super resolution microscopy.[13,16] While the mechanism of blinking is still unknown, a number of hypotheses have been presented.[18–22] For metal-enhanced fluorescence nanoparticles, recent research shows that the surface plasmon effect may play a role in some cases.[18,23,24]

Metal-enhanced fluorescence (MEF) is a widely studied phenomenon characterized by the increase in a fluorophore's emission intensity when in proximity to the surface of a metal nanostructure. The fluorescence emission results from the interaction with the surface plasmons of the metal nanostructure interacting with the excited fluorophore, resulting in an amplification of the fluorescence.[25–31] The MEF effect is dependent on several factors including nanoparticle size, material, and morphology, as well as the distance between the

Texas Tech University Department of Chemistry and Biochemistry, Lubbock, TX, USA. E-mail: d.pappas@ttu.edu

† Electronic supplementary information (ESI) available. See DOI: 10.1039/c9ra10421f

metal surface and the fluorophore.[25–28,30,31] It has been shown that fluorophores placed approximately 5 nm or less from the metal surface are quenched rather than enhanced, with 10 nm shown to be the optimum distance for MEF with enhancement decreasing at greater distances.[27,29]

It is important to note that the fluorescence intensity will only be enhanced if there is a spectral overlap between the fluorophore excitation/emission range and the surface plasmon resonance band of the nanostructure.[29–31] MEF leads to alterations in the quantum yield (Q) and the fluorescence lifetime (τ) of the fluorophore as demonstrated by eqn (1)–(4) where Q is the quantum yield, τ is the fluorescence lifetime, Γ is the radiative decay rate, and k_{nr} is the non-radiative decay rate. Eqn (1) and (2) give the fluorescence behavior of non-metal enhanced fluorophores and eqn (3) and (4) represent a fluorophore experiencing MEF; these equations are derived by treating the metal nanostructure and fluorophore as a coupled system.[27]

$$Q_0 = \Gamma_0 \tau_0 \quad (1)$$

$$\tau_0 = \frac{1}{\Gamma + k_{nr}} \quad (2)$$

$$Q_m = \frac{\Gamma_0 + \Gamma_m}{\Gamma_0 + \Gamma_m + \Gamma_{nr} + k_{nr}} \quad (3)$$

$$\tau_m = \frac{1}{\Gamma_0 + \Gamma_m + \Gamma_{nr} + k_{nr}} \quad (4)$$

In this work we investigate the role of core and shell size, and nanoparticle concentration on blinking of Rhodamine 110 (R110) doped Ag@SiO_2 core–shell fluorescent nanoparticles (Fig. 1). We observed that the silver cores are responsible for blinking, as the bare cores exhibited weak, blinking luminescence. Adding shells with doped dyes increase intensity and allow tuning emission wavelengths. Changes in core size did not result in a statistically different intensity of blinking duty cycle, indicating that core–shell nanoparticles can be optimized for smaller size without compromising blinking behavior for super-resolution microscopy.

Materials and methods

Reagents

Ethanol was purchased from Greenfield Global. Silver nitrate was purchased from Alfa Aesar. Tetraethoxysiloxane (TEOS) was purchased from Acros Organics and ammonium hydroxide was purchased from Thermofisher Scientific. Rhodamine 110 and sodium chloride were purchased from Sigma-Aldrich.

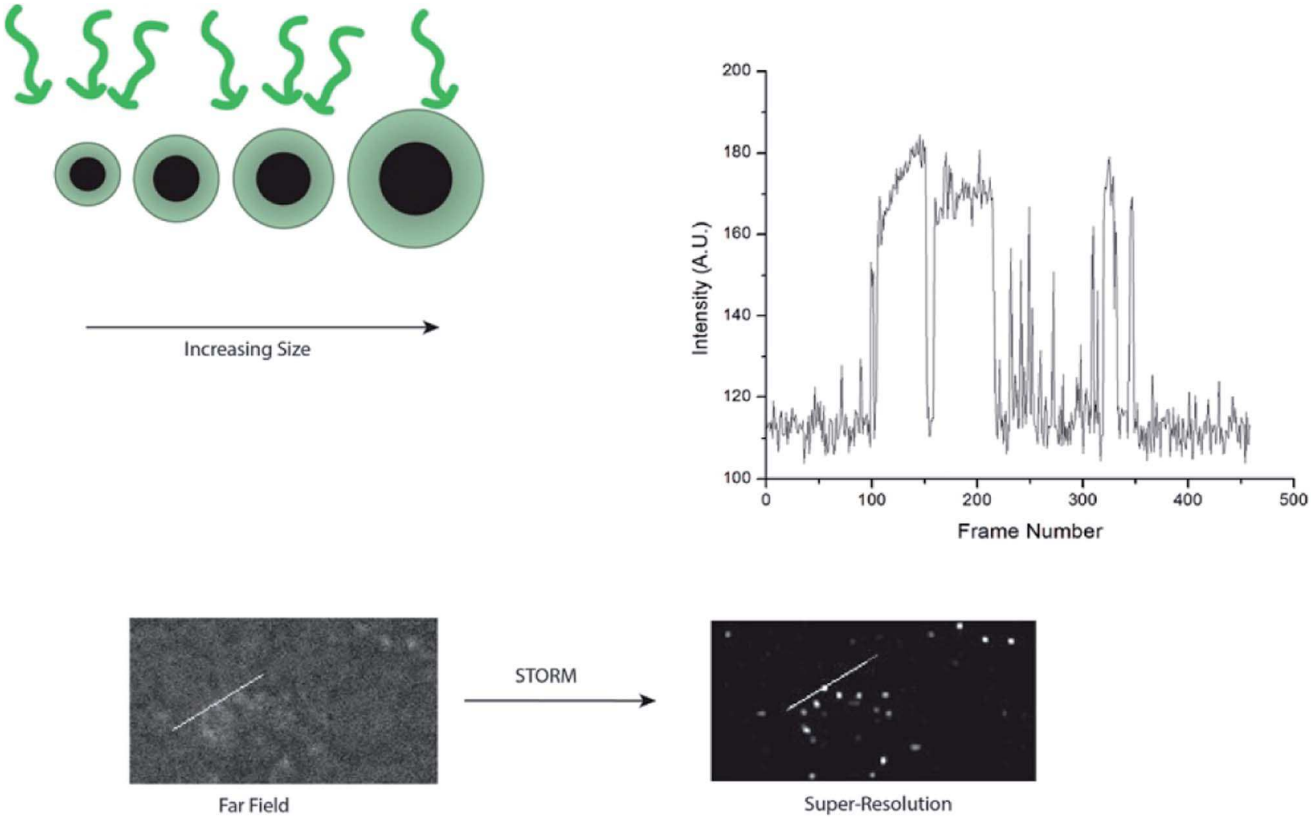

Fig. 1 Schematic of the experimental process. Metal-enhanced fluorescence nanoparticles of differing core and shell sizes were synthesized. The intensity and duty cycle of the "on" states of nanoparticle blinking were measured for each set of synthesis conditions. The process was used to optimize particle size for super-resolution imaging through STochastic Optical Reconstruction Microscopy (STORM). In addition to particle size, the effects of hydration and concentration of the nanoparticles were investigated.

Fabrication of the nanoparticle cores

To fabricate the nanoparticle cores, 50 mL of aqueous silver nitrate (concentration 9 mg : 50 mL) was heated to boiling in a 250 mL Erlenmeyer flask. Upon boiling, 1 mL of aqueous trisodium citrate (concentration 10 mg : 1 mL) was added and the reaction solution was stirred using a magnetic stir bar at a rate of 140 rpm for 1–10 min. The solution was then allowed to cool to room temperature. The size of the cores was tuned *via* the reaction time.

Fabrication of the nanoparticle shell

Nanoparticle shells were synthesized *via* a modified Stober synthesis.[32] Nanoparticle cores were suspended in a mixture of 200 mL 95% ethanol and 4 mL of ammonium hydroxide. 10 mL of tetraethoxysiloxane (TEOS) diluted in ethanol (concentration

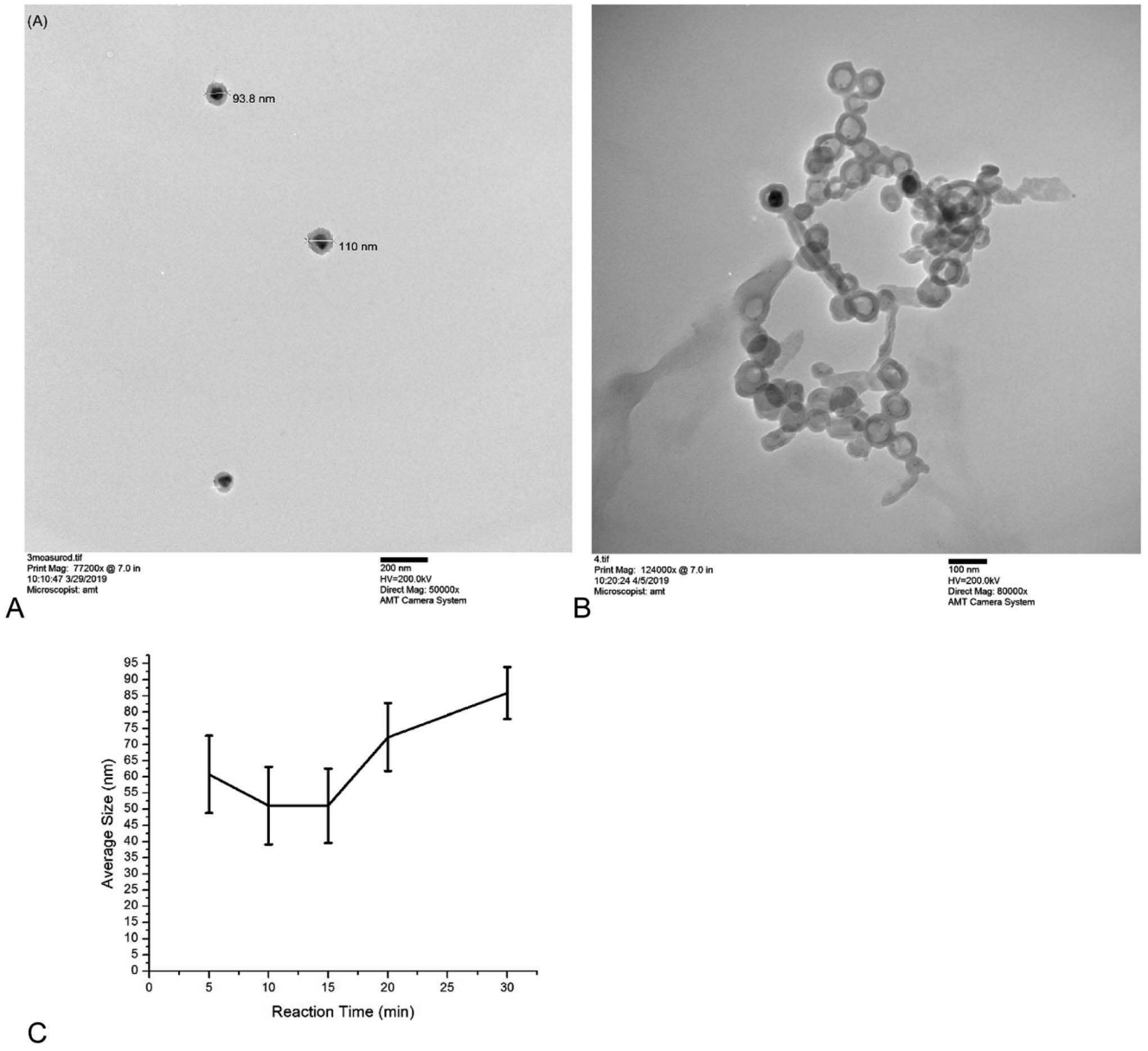

Fig. 2 (A) TEM image of the representative nanoparticles showing the shape of the particles and size measurements of two particles. The core–shell structure of the nanoparticles is clearly shown, with the solid core being shown as black and the sol–gel shell being shown as grey. The circularity of the nanoparticles was 0.97 ± 0.06 (B) TEM image of the nanobubble controls under higher magnification. The darker grey areas are due to overlap of the nanobubbles rather than cores, however there were some nanobubbles with most of their core present (black spots) likely due to insufficient time in the sodium chloride solution; there are clearly far more nanobubbles without cores than there are with cores. The nanobubbles have a slightly irregular shape due to a lack of a solid, regularly shaped core to support the more flexible sol–gel (circularity $= 0.87 \pm 0.05$). Differences in circularity between nanoparticles and nanobubble controls was statistically significant ($p = 0.008$). The effect of reaction time on core size (C) did not yield statistically different core sizes. The particle size measurements of the 5 minute reaction time is skewed in part by the small number of cores synthesizes at the reaction condition. The error is the full width at half maximum of the Gaussian curve generated from the dynamic light scattering data and the average is the maximum value of the Gaussian curve.

22.5 mL : 10 mL) was added dropwise for the next four hours while the reaction solution was stirred using a magnetic stir bar at a rate of 140 rpm. Rhodamine 110 dye was added to the reaction solution only in the final, optimized nanoparticle. After four hours, the stirring and addition of TEOS were stopped and the solution sat undisturbed for several hours while the silica deposited on the cores.

Fabrication of the nanobubble control

The fluorescent nanoparticle was synthesized as described above, after which 500 μL of the nanoparticle solution was reacted with 48 mg of sodium chloride for 24 hours to remove the silver cores.[33]

Characterization of the nanoparticles

To perform fluorescence microscopy measurements 1–3 drops of nanoparticle solution were dried onto a glass slide under a fume hood at room temperature and excited by green light (wavelength 562 nm) using an Olympus IX51 microscope with a 60× (NA = 0.6) dry objective. Videos were recorded using a sCMOS camera with a pixel size of 5 × 5 μm (Quantalux, ThorLabs or EDGE, PCO). The effective pixel size varied with the sCMOS sensor used. To observe the nanoparticles in a hydrated environment several drops of PBS buffer were placed over the dried nanoparticles prior to analysis.

The nanoparticle core size distribution measurements were performed using Dynamic Light Scattering (DLS) (Zetatrac Particle Size Analyzer, Malvern Inc.). The final, optimized nanoparticles were imaged using a transmission electron microscope (TEM) (Hitachi H8 100 TEM microscope) in order to determine the thickness of the silica sol–gel shell and the diameter of the core–shell nanoparticles.

Data analysis

Fluorescence microscopy measurements were conducted by obtaining image sequences stored as raw TIFF images. The image sequences were analyzed using ImageJ software to obtain peak intensity and duty cycle of the "on" states. The threshold to reject background noise was calculated using the following equation.

$$\text{Threshold} = \bar{x} + 3\sigma \quad (5)$$

The average ($\bar{x}$) and standard deviation (σ) of an area of the image sequence where the nanoparticle is in an "off" state was taken to find the threshold using eqn (5). The duty cycle – the percentage of time the nanoparticle was in an "on" state – of each nanoparticle was determined using the following equation.

$$\text{DC}\% = \frac{\text{on frames}}{\text{total frames}} \times 100 \quad (6)$$

The number of frames with the nanoparticle in the "on" state was determined using Excel's countif function. To verify single particle imaging, super-resolution localization using the ThunderSTORM ImageJ plugin was used to compute the centroid of local neighborhoods.[2]

Results and discussion

Physical characterization and effects of reaction time on core size

Core–shell nanoparticles were observed to be spherical with uniformly thick shells by TEM (Fig. 2A). The circularity of the nanoparticles was determined from TEM images to be 0.97 ± 0.06 (n = 10). Nanoparticles with etched cores (nanobubbles) served as controls to ensure the blinking and brightness of the nanoparticle are not due to dye aggregation in the sol–gel layer (Fig. 2B). Nanobubbles were not as regularly shaped, due to the lack of a core to support the sol–gel layer (circularity = 0.87 ± 0.05, n = 10). The differences in the circularity of the nanoparticles and the nanobubbles was statistically significant, with a p-value of 0.008. With the exception of the five-minute reaction time (Fig. 2C), increasing the reaction time increased core size, which was expected. The five-minute reactions yielded a small number of particle cores, which may result in skewed results in the dynamic light scattering measurements.

The fluorescence spectra for the bare cores, sol–gel clad cores, and fully-synthesized nanoparticle containing dye are shown in Fig. 3. The Ag cores exhibit weak, blinking photoluminescence. The sol–gel clad nanoparticles lacking Rhodamine 110 show a similar spectrum, although the emission intensity is slightly increased. The fully-synthesized core–shell particle containing Rhodamine 110 shows a significantly brighter a blue-shifted fluorescence than the core of core–shell lacking dye.

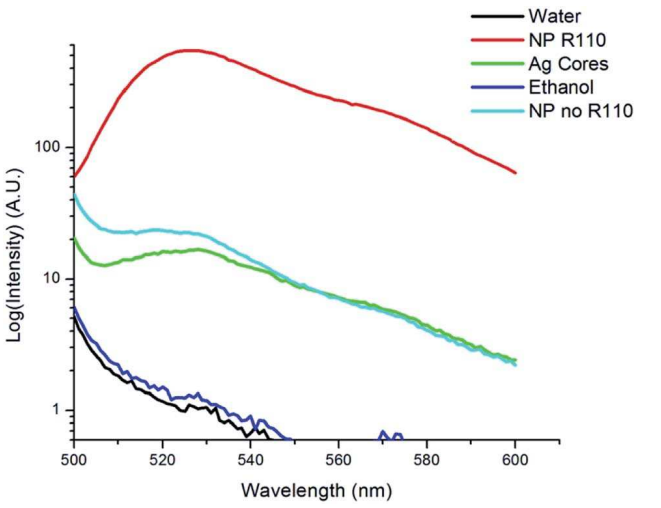

Fig. 3 Fluorescence spectra of the complete nanoparticle (NP R110), the nanoparticle without dye (NP no. R11), the bare silver cores, a water blank, and an ethanol blank. The spectra have been plotted on a base 10 log scale. The complete nanoparticle has the highest fluorescence intensity, and the bare cores and nanoparticle without dye have similar spectra to each other. There is also a blue shift in the emission of the final nanoparticle relative to the bare core.

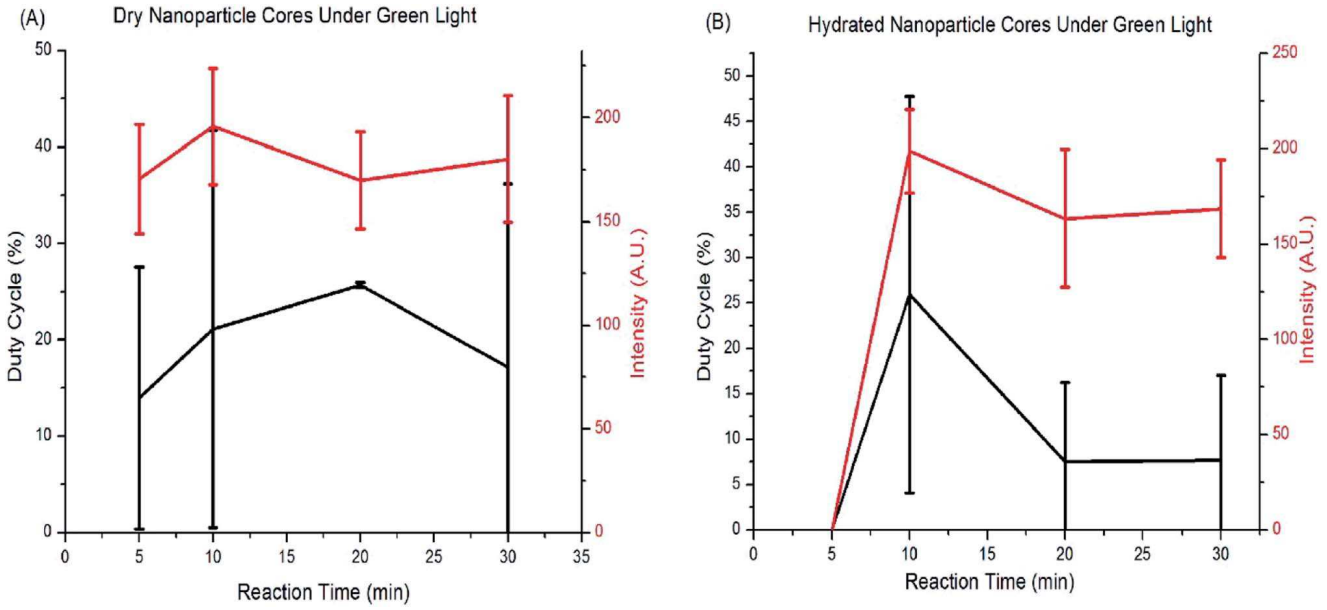

Fig. 4 The duty cycle and intensity of the bare cores plotted as a function of reaction time while (A) dry and (B) hydrated. There is no statistical difference between the duty cycles and intensities of the different sized cores and no trend in their fluorescence behavior for either (A) dry or (B) hydrated conditions. Cores were therefore chosen for the smallest size that still yielded high luminescence intensity under hydrated conditions.

Core optimization for photoblinking

The silver cores synthesized with differing reaction times were analyzed by fluorescence microscopy and found to be weakly fluorescent without the shell or added dye (Fig. 4). Analysis of the image sequences revealed that the duty cycle and luminescence intensity of the cores was tunable with core size. Fig. 4 shows a graph of the duty cycle and fluorescence intensity for each core reaction time when excited under green light (562 nm). There is no statistical difference in fluorescence and photoblinking behavior with core reaction time, and no trend in their behavior, so the cores chosen for the next round of experiments were the ones with the smallest size and highest luminescence intensity under hydrated conditions. The 10 minute cores are the smallest that can be synthesized before fluorescence decreases under hydrated conditions.

Core size was also tuned by reducing the citrate concentration or by sodium dodecyl sulfate (SDS), and by modification of the synthesis procedure used by Shah, *et al.*[34] Table 1 summarizes reaction conditions and their impact on blinking. The cores synthesized using lower concentrations of trisodium citrate showed faint fluorescence but no photoblinking. The nanoparticle cores limited in size by SDS showed fluorescence

Table 1 The effect of synthesis conditions on the native luminescence and blinking of reduced silver cores. Unless otherwise specified, the reaction conditions are as follows: trisodium citrate: 10 mg; silver nitrate: 9 mg; SDS: concentration – 35 mM; total reaction volume 50 mL reaction mixture heated to boiling. (*) Unable to obtain accurate size measurements due to the small number of nanoparticles present

Reaction time/conditions	Core size (nm)	Luminescence	Blinking observed
30 min dry	85.9 ± 8	Y	Y
30 min hydrated	85.9 ± 8	Y	Y
20 min dry	72.3 ± 10.5	Y	Y
20 min hydrated	72.3 ± 10.5	Y	Y
10 min dry	51.1 ± 12	Y	Y
10 min hydrated	51.1 ± 12	Y	Y
5 min dry	60.8 ± 12	Y	Y
5 min hydrated	60.8 ± 12	N	N
5 min 10× citrate dilution, dry	*	Y	N
5 min 10× citrate dilution, hydrated	*	N/A	N/A
5 min 5× citrate dilution, dry	*	Y	N
5 min 5× citrate dilution, hydrated	*	N/A	N/A
30 min 1 mL SDS, dry	*	Y	Y (faint)
30 min 1 mL SDS, hydrated	*	N/A	N/A
1 h 5 mL SDS 90 °C, dry	*	Y	N
1 h 5 mL SDS 90 °C, hydrated	*	N/A	N/A

Table 2 Summary of the shell thickness modification experiment results. Unless otherwise specified, the reaction conditions are as follows: TEOS – 22.5 μL; Rhodamine 110 – 80 μL of 1 mM solution or saturated solution. Unless otherwise specified, the shell was formed on to the 10 minute cores. As stated in the table, in some conditions fluorescence was only observed when nanoparticles formed aggregates

Reaction time/conditions	Dye	Fluorescence	Photoblinking
10 h dry	N	Y	Y
10 h hydrated	N	Y	Y
8 h dry	N	Y	Y
8 h hydrated	N	Y	Y
6 h dry	N	Y	Y
6 h hydrated	N	Y	Y
4 h dry	N	Y	Y
4 h hydrated	N	Y	Y
2 h dry	N	Y	Y
2 h hydrated	N	Y	Y
2 h dry	Y	Y	Y
2 h hydrated	Y	Y	Y
2 h 5× citrate dilution core, dry	Y	At aggregates	N
2 h 5× citrate dilution core, hydrated	Y	At aggregates	N
2 h 10× citrate dilution core, dry	Y	At aggregates	N
2 h 10× citrate dilution core, hydrated	Y	At aggregates	N
2 h 1 mL SDS core, dry	Y	At aggregates	N
2 h 1 mL SDS core, hydrated	Y	At aggregates	N
2 h 5 mL SDS core, dry	Y	N	N
2 h 5 mL SDS core, hydrated	Y	N/A	N/A

and blinking was observed for a small number of nanoparticles. The nanoparticles synthesized using a modification of Shah's synthesis procedure showed fluorescence but no blinking. Both dry and hydrated cores were tested. Based on our observation, there appears to be a limit to making smaller cores while retaining blinking behavior, but this could be due in part to a small number of cores synthesized under those conditions.

Effects of silica shell thickness

Shell thickness impacts the dye loading, dye-core distance, and the overall particle size (Table 2). 10 minute cores (51.1 ± 12 nm) were used for all shell studies. Fig. 5 show histograms of duty cycle of the core–shell nanoparticle blinking. The variance in duty cycles for a given set of synthesis conditions is large enough that there is not a significant difference in the blinking duty cycle with core thickness. Blinking in hydrated conditions was the parameter used to assess nanoparticle behavior, as these particles will ultimately be used in aqueous systems. Therefore, the smallest nanoparticle shell was chosen in order to take advantage of localization in super-resolution microscopy.

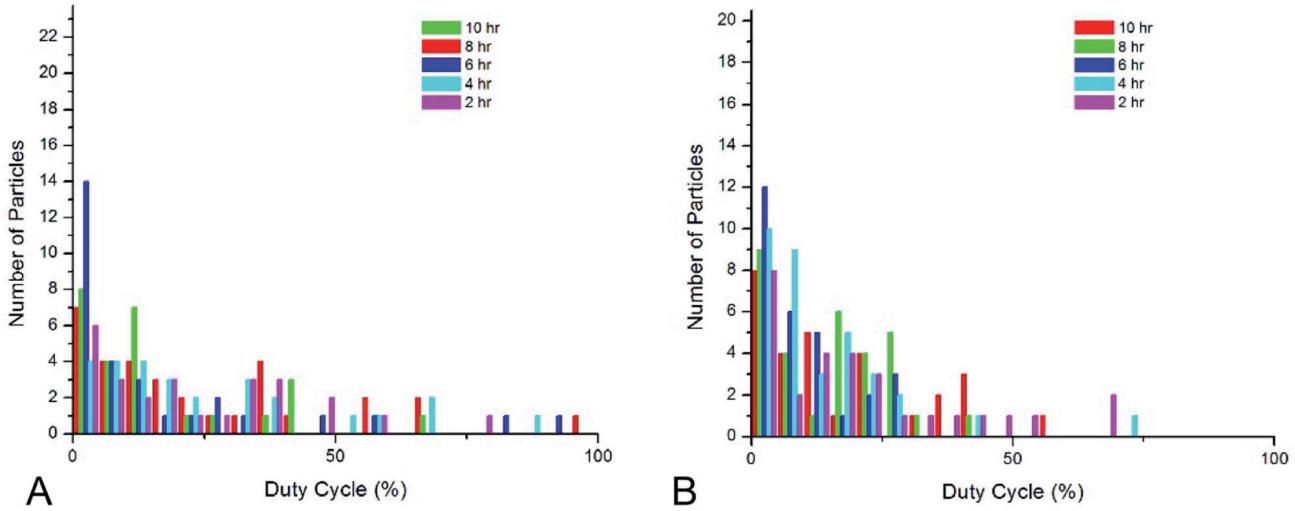

Fig. 5 The behavior of the core–shell nanoparticle without dye when (A) dry and (B) hydrated. There is no statistical difference in fluorescence intensity and duty cycle for either dry or hydrated nanoparticles and no clear trend under hydrated conditions, therefore the chosen shell thickness was based solely on shell thickness to have the smallest nanoparticle possible.

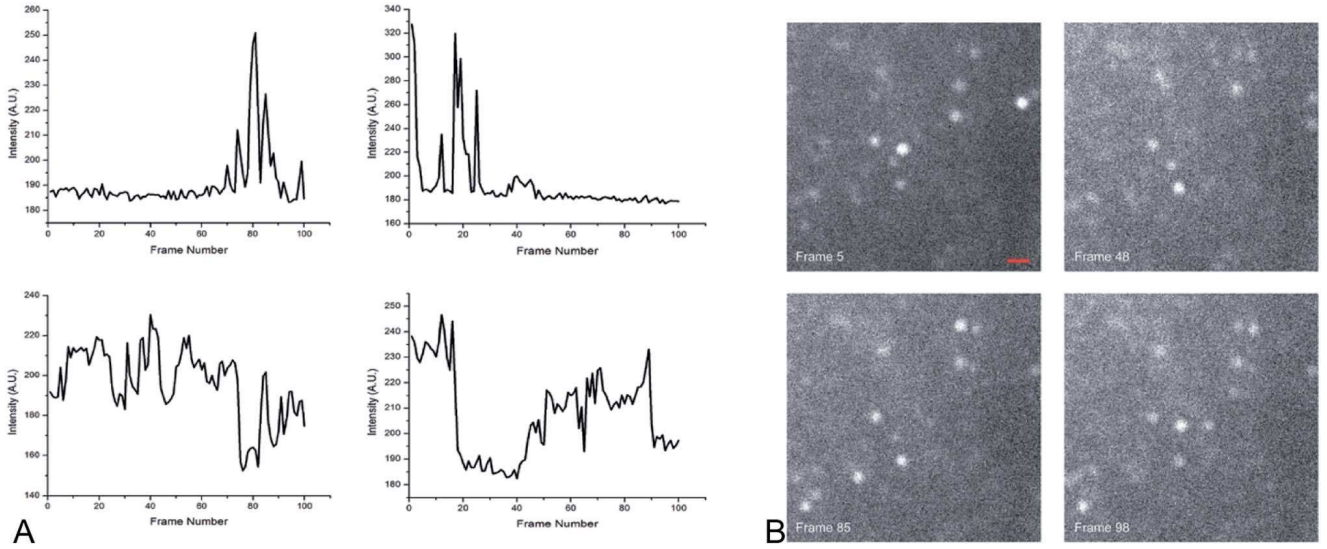

Fig. 6 (A) Blinking behavior from several representative nanoparticles, showing clear periods of "on" and "off" states. (B) Four frames from an image sequence of metal-enhanced nanoparticle fluorescence. The "on"–"off" state changes are clearly visible for several nanoparticles. Scale bar = 1.8 μm.

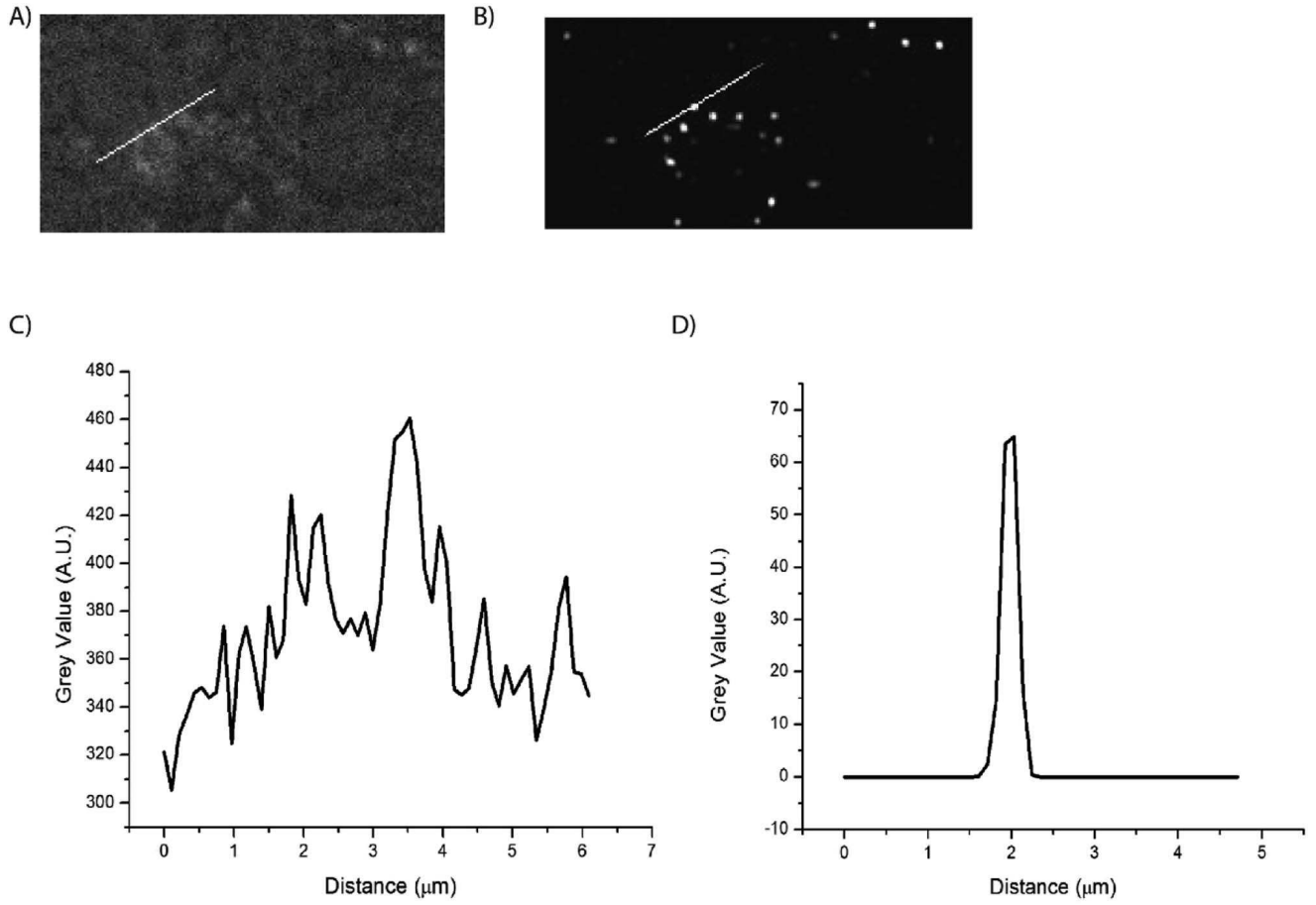

Fig. 7 Super-resolution localization of blinking nanoparticles. The far-field (A) and super-resolution (B) images show a clear improvement in spatial resolution. Line scans of the far-field (C) and super-resolution (D) images. Line scans of the image show nanoparticle sizes of 270 nm, which approaches the dynamic light scattering size data. As the particle size does not significantly impact blinking properties, the smallest nanoparticles can be synthesized to optimize super-resolution labeling.

Blinking behavior of optimized nanoparticles

The optimized nanoparticle had a total size of 80–110 nm. The duty cycle of the nanoparticles had a large variance (2–70% when hydrated), which is consistent with stochastically-behaving particles. It is worth noting that the blinking was rapid and required an increase in camera frame rate to temporally resolve the changes. Dye concentration effects were not studied because previous work had determined there was no statistical difference in duty cycle with changing dye concentration.[1] Fig. 2 shows a TEM image of the optimized nanoparticle, confirming DLS measurements of particle size and showing regularly-shaped particles based on circularity measurements. Fig. 6 shows the change in intensity of a representative nanoparticle undergoing blinking, as well as four image frames showing the "on" and "off" states.

Because the core size and shell thickness did not significantly impact the blinking behavior or fluorescence intensity, we were able to focus on tuning the nanoparticle for optimal size without risking the loss of the desired fluorescence and blinking behaviors.

In order to determine if nanoparticle concentration, and therefore proximity, plays a role in the photoblinking behavior of the nanoparticles a solution of nanoparticles was concentrated down to 1 mL, and performed four 10-fold dilutions were prepared from this stock. The true concentration of the nanoparticles is difficult to calculate or measure directly. It was observed that with each 10-fold dilution the fluorescence became less intense and the blinking became less frequent; nothing was observed in solutions 3 and 4 (the videos are provided in the ESI†). The proximity effect to the fluorescence and blinking behavior of the nanoparticles will be studied further in future work, as they may be harnessed in some conditions to study labeling density.

Super-resolution microscopy of single particles

Super-resolution microscopy was used to verify that we were imaging single particles rather than clusters of particles. STochastic Optical Reconstruction Microscopy (STORM) was used to localize the particles below the diffraction limit.[2] The pixel size of the system was 6.5 μm × 6.5 μm effective pixel size of the system was 0.108 μm. In order to localize the emitting, blinking particles, the image sequences were analyzed using the ThunderSTORM ImageJ plugin, which provides sub-diffraction limit localization of particles by computing the centroid of local neighborhoods.[2] Fig. 7 shows the super-resolution images of blinking nanoparticles, with a line scan across a representative particle shown in Fig. 6C.

Conclusions

Here we presented Rhodamine 110 doped Ag@SiO_2 core–shell nanoparticles tailored to exhibit optimal blinking behavior at smaller particle sizes. The blinking behavior was tuned by altering the size or the nanoparticle cores and shells. By reducing the size of the Ag core and the thickness of the SiO_2 shell we were able to increase the rate of blinking by the nanoparticles, as compared to the previously studied nanoparticles. This improved blinking behavior will lead to better localization precision and will allow the nanoparticles to be used as fluorescent probes in super-resolution fluorescence microscopy.[16]

Additionally, the bare nanoparticles were found to blink, and that this blinking was impacted by solvation. The fluorophores themselves to not inherently blink. The fully-synthesized particle gains its strong intensity from the core plasmon. This blinking of the core therefore modulates the amplification effect of the metal enhanced nanoparticle.

Conflicts of interest

The authors declare no conflicts of interest.

Acknowledgements

This work was supported in part by grants from the National Institutes of Health (GM120669) and the National Science Foundation (CBET 1849063). Dynamic Light Scattering measurements were performed at the Texas Tech University Materials Characterization Center. TEM analysis was performed at the Texas Tech University Imaging Center.

References

1 C. Chakraborty, S. Thompson, V. J. Lyons, C. Snoeyink and D. Pappas, Modulation and study of photoblinking behavior in dye doped silver-silica core-shell nanoparticles for localization super-resolution microscopy, *Nanotechnology*, 2019, **30**(45), 455704.
2 M. Ovesny, P. Krizek, J. Borkovec, Z. Svindrych and G. M. Hagen, ThunderSTORM: a comprehensive ImageJ plug-in for PALM and STORM data analysis and super-resolution imaging, *Bioinformatics*, 2014, **30**(16), 2389–2390.
3 M. J. Rust, M. Bates and X. Zhuang, Sub-diffraction-limit imaging by stochastic optical reconstruction microscopy (STORM), *Nat. Methods*, 2006, **3**(10), 793–795.
4 J. Tam and D. Merino, Stochastic optical reconstruction microscopy (STORM) in comparison with stimulated emission depletion (STED) and other imaging methods, *J. Neurochem.*, 2015, **135**(4), 643–658.
5 L. Valiya Peedikakkal, V. Steventon, A. Furley and A. J. Cadby, Development of targeted STORM for super resolution imaging of biological samples using digital micro-mirror device, *Opt. Commun.*, 2017, **404**, 18–22.
6 N. P. Brawand, M. Voros and G. Galli, Surface dangling bonds are a cause of B-type blinking in Si nanoparticles, *Nanoscale*, 2015, **7**(8), 3737–3744.
7 X. Chen, Z. Liu, R. Li, C. Shan, Z. Zeng, B. Xue, W. Yuan, C. Mo, P. Xi, C. Wu and Y. Sun, Multicolor Super-resolution Fluorescence Microscopy with Blue and Carmine Small Photoblinking Polymer Dots, *ACS Nano*, 2017, **11**(8), 8084–8091.
8 H. He, X. Liu, S. Li, X. Wang, Q. Wang, J. Li, J. Wang, H. Ren, B. Ge, S. Wang, X. Zhang and F. Huang, High-Density Super-

Resolution Localization Imaging with Blinking Carbon Dots, *Anal. Chem.*, 2017, **89**(21), 11831–11838.

9 Z. Liu, J. Liu, Z. Sun, Z. Zhang, Y. Yuan, X. Fang, F. Wang, W. Qin and C. Wu, Cooperative Blinking from Dye Ensemble Activated by Energy Transfer for Super-resolution Cellular Imaging, *Anal. Chem.*, 2019, **91**(6), 4179–4185.

10 F. Cannone, G. Chirico, A. R. Bizzarri and S. Cannistraro, Quenching and blinking of fluorescence of a single dye molecule bound to gold nanoparticles, *J. Phys. Chem. B*, 2006, **110**(33), 16491–16498.

11 H. He, X. Liu, S. Li, X. Wang, Q. Wang, J. Li, J. Wang, H. Ren, B. Ge, S. Wang, X. Zhang and F. Huang, High-Density Super-Resolution Localization Imaging with Blinking Carbon Dots, *Anal. Chem.*, 2017, **89**(21), 11831–11838.

12 S. N. Uno, M. Kamiya, A. Morozumi and Y. Urano, A green-light-emitting, spontaneously blinking fluorophore based on intramolecular spirocyclization for dual-colour super-resolution imaging, *Chem. Commun.*, 2017, **54**(1), 102–105.

13 J. Vogelsang, C. Steinhauer, C. Forthmann, I. H. Stein, B. Person-Skegro, T. Cordes and P. Tinnefeld, Make them blink: probes for super-resolution microscopy, *ChemPhysChem*, 2010, **11**(12), 2475–2490.

14 X. Wu and E. K. Yeow, Fluorescence blinking dynamics of silver nanoparticle and silver nanorod films, *Nanotechnology*, 2008, **19**(3), 035706.

15 Z. Sun, Z. Liu, H. Chen, R. Li, Y. Sun, D. Chen, G. Xu, L. Liu and C. Wu, Semiconducting Polymer Dots with Modulated Photoblinking for High-Order Super-Resolution Optical Fluctuation Imaging, *Adv. Opt. Mater.*, 2019, **7**, 65701.

16 S. Zong, F. Pan, R. Zhang, C. Chen, Z. Wang and Y. Cui, Super blinking and biocompatible nanoprobes based on dye doped BSA nanoparticles for super resolution imaging, *Nanotechnology*, 2018, **30**, 6.

17 B. Zhi, Y. Cui, S. Wang, B. P. Frank, D. N. Williams, R. P. Brown, E. S. Melby, R. J. Hamers, Z. Rosenzweig, D. H. Fairbrother, G. Orr and C. L. Haynes, Malic Acid Carbon Dots: From Super-resolution Live-Cell Imaging to Highly Efficient Separation, *ACS Nano*, 2018, **12**, 5741–5752.

18 X. W. Wu, M. Gong, C. H. Dong, J. M. Cui, Y. Yang, F. W. Sun, G. C. Guo and Z. F. Han, Anti-bunching and luminescence blinking suppression from plasmon-interacted single CdSe/ZnS quantum dot, *Optic Express*, 2010, **18**(6), 6340–6346.

19 J. Schuster, F. Cichos and C. v. Borezyskowski, Blinking of Single Molecules in Various Environments, *Opt. Spektrosk.*, 2005, **98**(5), 712–717.

20 J. Hofkens, T. Vosch, M. Maus, F. Kohn, M. Cotlet, T. Weil, A. Herrmann, K. Mullen and F. D. Schryver, Conformational rearrangements in and twisting of a single molecule, *Chem. Phys. Lett.*, 2001, **333**, 255–263.

21 E. K. Yeow, S. M. Melnikov, T. D. Bell, F. C. De Schryver and J. Hofkens, Characterizing the fluorescence intermittency and photobleaching kinetics of dye molecules immobilized on a glass surface, *J. Phys. Chem. A*, 2006, **110**(5), 1726–1734.

22 S. Wang, C. Querner, T. Emmons, M. Drndic and C. H. Crouch, Fluorescence blinking statistics from CdSe core and core/shell nanorods, *J. Phys. Chem. B*, 2006, **110**(46), 23221–23227.

23 X. Wu and E. K. Yeow, Fluorescence blinking dynamics of silver nanoparticle and nanorod films, *Nanotechnology*, 2008, **19**, 3.

24 C. D. Geddes, A. Parfenov, I. Gryezynski and J. R. Lakowicz, Luminescent Blinking from Silver Nanostructures, *J. Phys. Chem. B*, 2003, **107**, 9989–9993.

25 B. J. Yun, J. E. Kwon, K. Lee and W. G. Koh, Highly sensitive metal-enhanced fluorescence biosensor prepared on electrospun fibers decorated with silica-coated silver nanoparticles, *Sens. Actuators, B*, 2019, **284**, 140–147.

26 S. Iqbal, M. Shabaninezhad, M. Hatshan, P. M. Niraula, A. Abuhagr, H. Alali, R. Guda and A. Kayani, Ion-implanted silver nanoparticles for metal-enhanced fluorescence, *AIP Adv.*, 2018, **8**(9), 95217.

27 S. M. Fothergill, C. Joyce and F. Xie, Metal enhanced fluorescence biosensing: from ultra-violet towards second near-infrared window, *Nanoscale*, 2018, **10**(45), 20914–20929.

28 D. D. Xu, B. Zheng, C. Y. Song, Y. Lin, D. W. Pang and H. W. Tang, Metal-enhanced fluorescence of gold nanoclusters as a sensing platform for multi-component detection, *Sens. Actuators, B*, 2019, **282**, 650–658.

29 T. Ribeiro, C. Baleizao and J. P. S. Farinha, Artefact-free Evaluation of Metal Enhanced Fluorescence in Silica Coated Gold Nanoparticles, *Sci. Rep.*, 2017, **7**(1), 2440.

30 C. Xiao, Z. Cao, J. Deng, Z. Huang, Z. Xu, J. Fu and L. Yobas, Microfluidic-based metal enhanced fluorescence for capillary electrophoresis by Ag nanorod arrays, *Nanotechnology*, 2014, **25**(22), 225502.

31 O. G. Tovmachenko, C. Graf, D. J. v. d. Heuvel, A. v. Blaaderen and H. C. Gerritsen, Fluorescence Enhancement by Metal-Core/Silica-Shell Nanoparticles, *Adv. Mater.*, 2006, **18**, 91–95.

32 W. Zhang, Y. Tian, X. Hu, S. He, Q. Niu, C. Chen, S. Zhu and X. Yan, Light-Scattering Sizing of Single Submicron Particles by High-Sensitivity Flow Cytometry, *Anal. Chem.*, 2018, **90**(21), 12768–12775.

33 M. Dong, Y. Tian and D. Pappas, Synthesis of a red fluorescent dye-conjugated Ag@SiO_2 nanocomposite for cell immunofluorescence, *Appl. Spectrosc.*, 2015, **69**(2), 215–221.

34 V. Shah, B. Bharatiya, M. K. Mishra, D. Ray and D. O. Shah, Molecular insights into sodium dodecyl sulphate mediated control of size for silver nanoparticles, *J. Mol. Liq.*, 2019, **273**, 222–230.